Kinetics of the Subtransition in Dipalmitoylphosphatidylcholine†

S. Tristram-Nagle,* M. C. Wiener, C.-P. Yang, and J. F. Nagle

Departments of Biological Sciences and Physics, Carnegie Mellon University, Pittsburgh, Pennsylvania 15213

Received January 13, 1987; Revised Manuscript Received March 17, 1987

ABSTRACT: The kinetics of the interconversions of the subgel and gel phases in dipalmitoylphosphatidylcholine have been studied by using differential dilatometry, differential scanning calorimetry (DSC), and neutral buoyancy centrifugation as a function of incubation temperature and deuteriation of the solvent. As seen by others, DSC scans show two peaks in the subgel transition region for incubation temperatures below 1 °C. After incubation at 0.1 °C, the DSC peak that occurs at the lower scanning temperature appears with an incubation half-time of 0.5 day and eventually converts into a peak at higher scanning temperature with an incubation half-time of 18 days. By varying the scanning rate, we show that these two peaks merge into one at slow scanning rates with a common equilibrium transition temperature of 13.8 °C, in agreement with equilibrium calorimetry and dilatometry ($\Delta V = 0.017 \pm 0.001$ mL/g). For incubation temperatures above 4.6 °C, only one peak appears in both scanning dilatometry and calorimetry. While the initial rate of subgel conversion is smaller at the higher incubation temperatures, after 300 h a higher percentage of the sample has converted to subgel than at the lower incubation temperatures. We suggest that higher incubation temperatures (near 5 °C) are preferable for forming the stable subgel phase, and we present a colliding domain picture that indicates why this may be so. Our results in D_2O and the similarity of the kinetics of volume decrease with the kinetics of wide-angle diffraction lines also support the suggestion that the partial loss of interlamellar water plays a kinetic role in subgel formation.

Considerable research has focused upon the relatively recently discovered phospholipid subtransition (Chen et al., 1980) between the gel phase (G or $L_{\beta'}$ phase)[1] and the low-temperature ordered phase (C or $L_{c'}$ subgel phase) that exists below this transition (Nagle & Wilkinson, 1982; Cameron & Mantsch, 1982; Finegold & Singer, 1984, 1986; Serrallach et al., 1984; Ter-Minassian-Saraga & Madelmont, 1984; Singer & Finegold, 1985; Silvius et al., 1985; Kodama et al., 1985; Wilkinson & McIntosh, 1986). Since it forms a more highly ordered crystalline form than the gel phase, X-ray diffraction of the C phase produces many sharp reflections (Fuldner, 1981; Ruocco & Shipley, 1982a,b). Using this technique, Church et al. (1986) have determined the unit cell dimensions for DPPC and some isobranched lipids, and Blaurock and McIntosh (1985) have determined the unit cell for dipalmitoylphosphatidylglycerol. Thus, the detailed bilayer structure and packing of the lipid molecules are better known for the C phase than for the other phases, especially when diffraction results are coupled with absolute specific volumes (Yang et al., 1986; Wiener et al., 1987). It is then possible to use the results for the relatively well-determined C phase to improve the characterization of the higher temperature lipid bilayer phases. Two examples of how such a procedure has been utilized, starting from the less completely characterized G phase rather than the C phase and going to the fluid liquid-crystalline phase, are given by Nagle and Wilkinson (1978) and McIntosh and Simon (1986).

One complication regarding C-phase formation has emerged recently. The original data on DPPC (Chen et al., 1980; Nagle & Wilkinson, 1982) indicated that the subtransition consisted of one moderately broad endotherm, but with the availability of purer lipids, DSC data have shown two or more peaks in DPPC (Wu et al., 1985; Silvius et al., 1985; Tristram-Nagle & Nagle, 1986) and in C_{17}PC (Finegold & Singer, 1984). This suggests, at least superficially, that there may be more than one C phase. In order to accomplish the goals of the first paragraph, it is crucial that any multiplicity of phases be sorted out and any comparison of data from different experiments be for the same C phase. Although investigations of the subgel are lengthy due to the long incubation times at low temperatures required for its formation, the C phase is ideally suited to a detailed analysis of a lipid phase transformation since the kinetics are slow enough to be monitored accurately. Incubating DPPC at various low temperatures in our dilatometer allows direct measurements of the volume changes that occur in the lipid during C-phase formation. Both dilatometry and calorimetry were used in this study to understand the differences between the two subgel peaks.

Since this paper deals with the kinetics of the subtransition, it is essential that the direction of the transition be clearly described, and it is useful to do so with brief names. Accordingly, we will use the word "formation" to describe the phase transformation from the gel phase to the subgel phase and the word "melting" to describe the phase transformation from the subgel phase to the gel phase. The reader should not confuse this use of the term "melting" with the DPPC main chain melting transition at 41.4 °C.

Materials and Methods

Lyophilized DPPC was obtained from Avanti Polar Lipids (Birmingham, AL) and was used as received. The primary check of purity was the calorimetrically determined small half-width of the main transition (between 0.08 and 0.12 °C). Lipid purity was also checked by TLC using the solvent system chloroform/methanol/water in volume ratios 60:30:5. DPPC

† This research was supported by NIH Grant GM21128.

* Address correspondence to this author at the Department of Biological Sciences, Carnegie Mellon University.

[1] Abbreviations: DPPC, 1,2-dipalmitoyl-*sn*-glycero-3-phosphocholine; TLC, thin-layer chromatography; C phase, $L_{c'}$ or crystalline subgel phase; G phase, $L_{\beta'}$ or gel phase; DSC, differential scanning calorimetry.

0006-2960/87/0426-4288$01.50/0

was judged to be chromatographically pure by TLC, since only a single spot was detected with iodine after migration at 2–3 μmol loading of the lipid sample.

Sample Preparation. Multilamellar vesicles were prepared for DSC and dilatometry by first drying the lipid in a vacuum oven at 65 °C overnight, weighing, and then adding distilled water or D_2O (Aldrich Chemical Co., Milwaukee, WI) for some DSC experiments. The sample temperature was repeatedly (5 times) alternated between 60 and 0.1 °C, holding for 10 min and vortexing at each temperature. For calorimetry, the hydrated lipid was prepared either as a stock solution from which 0.916-mL aliquots were taken or in individual test tubes from which the entire lipid sample was transferred into the calorimeter using two washes with distilled water. For dilatometry, the samples were exhaustively degassed at room temperature under partial vacuum, while for calorimetry 5 min of degassing was sufficient.

Any degradation of the samples was ascertained by the same two criteria of purity stated earlier. Also, the pretransition of a DPPC sample kept several months in the dilatometer had the same half-width as a freshly loaded sample. When removed from the dilatometer and freeze-dried, the sample migrated as a single spot on TLC.

Dilatometry. The differential dilatometer has been described previously (Wilkinson & Nagle, 1978). In addition to being able to perform both heating and cooling scans, this instrument can maintain constant temperature (±0.005 °C) for extended times to allow monitoring of volume changes at one temperature. The thermistor probe used to monitor the temperature has been calibrated against platinum resistance and mercury thermometers certified by the National Bureau of Standards. The calibration points were combined with data for the thermistor probe supplied by Yellow Springs Instruments (Yellow Springs, OH) for the final thermistor calibrations.

Neutral Buoyancy Centrifugation. Determinations of the absolute specific volumes of DPPC were carried out by ultracentrifugation at 50000*g* at 5 °C for 1 h or in a desk-top centrifuge at 1000*g* for 3–4 h, at 4.6 ± 0.2 °C using D_2O/H_2O mixtures as described previously (Nagle & Wilkinson, 1978).

Calorimetry. A high-sensitivity differential scanning calorimeter, Microcal MC-1 (Microcal Inc., Amherst, MA), was used for the calorimetric measurements. An environmental chamber constructed of tightly wrapped refrigerated cooling coils within a styrofoam container allowed equilibration of the cells at 1–2 °C for unlimited time before low-temperature start-ups. The reference cell contained degassed distilled water or degassed D_2O for those lipid samples dispersed in D_2O. All data were collected in an Apple-II Plus computer and then transferred to an IBM PC. The PC converted the thermistor readings to temperatures using a calibration curve established previously by comparing transitions of lipid samples with dilatometry, where all transition temperatures were extrapolated to zero scan rate on both instruments. The calibration points were combined with data for the thermistor probes supplied by Yellow Springs Instruments for the final thermistor calibrations. The heating rates were obtained, and the data were converted to specific heats. Numerous calibrations of the specific heat scale have been carried out in two ways. In the first way, NaCl solutions (up to 20%) in the sample cell were scanned vs. pure water in the reference cell, and in the second way, a known amount of water was removed from the sample cell.

Subtraction of Base Lines. Base-line subtraction was required to integrate the area under the peaks. In order to assess the error involved in the base-line subtraction, three different methods were used (see Figure 1). Typical differences in transition enthalpy between different base-line subtraction methods were about 10% for subgel peaks with an initial upward slope as in Figure 1 and about 5% for other peaks. All transition enthalpies were calculated by using method B in Figure 1.

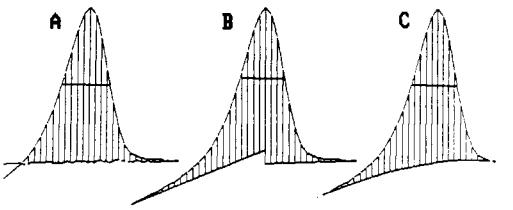

FIGURE 1: Three examples of ways to draw base lines with the resulting enthalpies of transition: (A) 2.2 kcal/mol; (B) 2.5 kcal/mol; and (C) 2.7 kcal/mol. The DSC scan of the transition was obtained from a sample of DPPC incubated for 1 day at 0.1 °C. The base line in (A) is the unincubated rescan of the sample, in (B), the base line is obtained by extending the slopes from both single-phase regions to the peak temperature, and in (C), a fifth order polynomial is fitted to the specific heat in the single-phase regions.

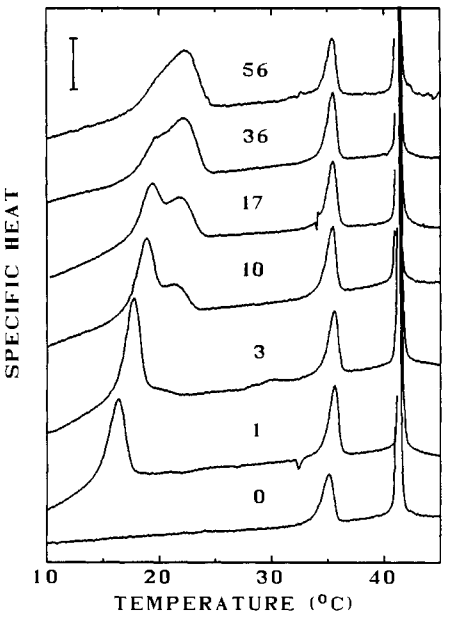

FIGURE 2: DSC scans of DPPC (3.1 mg/mL) incubated at 0.1 °C for the number of days indicated in the figure. Scan rate was 13.6 °C/h. The zero-day curve is the unincubated rescan of the sample that yielded the 36-day curve. The vertical bar indicates a specific heat of 1 cal/(deg·g).

Deconvolution and Integration. Following subtraction of a base line, the two peaks in the subgel region were first deconvoluted by using a computer program developed by C.-P. Yang. The program fitted two reference curves to the double-peaked spectra. The reference curves were DPPC samples incubated at 0.1 °C for (1) 1 day and (2) 128 days. The height, width, and peak temperatures of each reference curve could be varied until their sum gave the best fit to the data. (In practice, the width did not vary significantly.) The area under each reference curve was then computed.

RESULTS

Figure 2 shows DSC scans of DPPC incubated at 0.1 °C for different lengths of time. The chain melting main transition peak at 41.4 °C is essentially unaltered by low-temperature incubation. The pretransition peak near 35 °C is slightly sharper and has somewhat more enthalpy (ΔH_{pre} = 1.3 ± 0.1

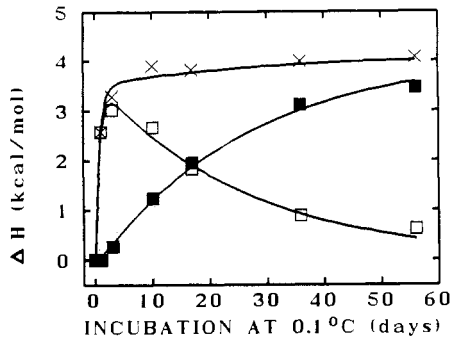

FIGURE 3: Subtransition enthalpies (kilocalories per mole) as a function of incubation time (in days) for the data shown in Figure 2. The total subtransition enthalpy is shown by time signs, the enthalpy under the first peak, ΔH_{C^*G}, is shown by open squares, and the enthalpy under the second peak, ΔH_{CG}, is shown by closed squares. The lines are the best least-squares fit to the data using the simple kinetic model described in the text.

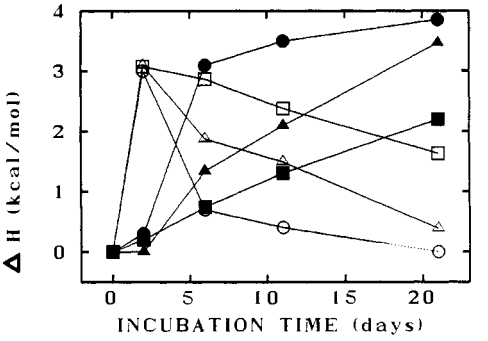

FIGURE 4: Subtransition enthalpies (kilocalories per mole) as a function of incubation time (in days) for additional incubation conditions: (squares) in H_2O, incubation temperature 0.1 °C; (circles) in H_2O, incubation temperature 0.1 °C for 1 day, 4.6 °C thereafter; (triangles) in D_2O, 0.1 °C for 1 day, 4.6 °C thereafter. Open symbols give the enthalpy under the lower temperature C*G peak, and closed symbols give the enthalpy under the higher temperature CG peak.

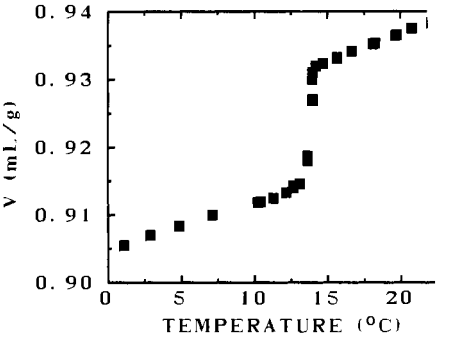

FIGURE 5: Equilibrium volume (milliliters per gram) vs. temperature (degrees centigrade) determined at each point by increasing the temperature and waiting until equilibrium was achieved as determined by no further volume change. In the center of the subtransition region, it was necessary to wait 4 days before no further change was seen. Overall scan rate in the transition region was 0.015 °C/h. The sample consisted of 0.199 g of DPPC (15 mg/mL) that had incubated at 0.8 °C for 10 days.

kcal/mol) when compared to no low-temperature incubation (ΔH_{pre} = 1.1 ± 0.1 kcal/mol). A delay of 1 day at room temperature between scanning the subtransition and scanning the pretransition still results in ΔH_{pre} = 1.3 kcal/mol. However, scanning through the pretransition, with or without scanning through the chain melting transition, is sufficient to reduce the pretransition enthalpy to 1.1 kcal/mol in subsequent scans.

These effects of incubation on the pretransition are minor when compared to the effects upon the endotherms at lower temperatures where the subtransition appears after 1 day of incubation as seen in Figure 2. For longer incubation times, it is apparent in the 10-, 17-, and 36-day curves in Figure 2 that there are two peaks below 30 °C instead of a single subtransition peak. While Figure 2 shows that the temperatures of both peaks increase with incubation time, it is also evident that the second peak grows at the expense of the first peak. This suggests that there are two low-temperature phases. These putative phases will be called C* and C, where C* is the phase which is first formed upon incubating the gel (G) phase and C is the ultimately stable crystal phase formed after long incubation times. The peak at lower temperatures will be called the C*G peak, and the one at higher temperatures will be called the CG peak.

Figure 3 shows the deconvoluted enthalpies, ΔH_{C^*G} and ΔH_{CG}, as well as the total enthalpy under both peaks as a function of incubation time. The data were fitted according to the simple first-order kinetics scheme G → C* → C upon incubation, for which

$$\Delta H_{C^*G}(t) = \Delta H_{C^*G}(\infty) \times [k_{GC^*}/(k_{GC^*} - k_{C^*C})]\,[\exp(-k_{C^*C}t) - \exp(-k_{GC^*}t)]$$

$$\Delta H_{CG}(t) = \Delta H_{CG}(\infty)\{1 - [k_{GC^*}/(k_{GC^*} - k_{C^*C})]\exp(-k_{C^*C}t) + [k_{C^*C}/(k_{GC^*} - k_{C^*C})]\exp(-k_{GC^*}t)\}$$

The resulting half-times were τ_{GC^*} = 0.53 day and τ_{C^*C} = 18 days, and the transition enthalpies were $\Delta H_{C^*G}(\infty)$ = 3.6 kcal/mol and $\Delta H_{CG}(\infty)$ = 4.1 kcal/mol. Figure 4 compares the kinetics of formation of the C* and C phases as determined by DSC for different incubation conditions. Compared to prolonged incubation at 0.1 °C, jumping the temperature to 4.6 ± 0.2 °C after 1 day increases the rate of conversion, roughly by a factor of 5. When the temperature jump experiment is carried out in D_2O instead of H_2O, the rate of conversion increases from the initial conditions by a factor of only 2.5, roughly half that in H_2O. However, there is no difference in these three cases in the rate of formation of the C* phase for the first 2 days of incubation.

Both peak temperatures, T_{C^*G} and T_{CG}, are higher from the DSC in Figure 2 than the subtransition temperature of 13.5 °C that has been reported by previous dilatometry from this lab (Nagle & Wilkinson, 1982) and by adiabatic calorimetry (Kodama et al., 1985). Since sample purity has improved, it is important to repeat the dilatometry. The data in Figure 5 confirm the earlier result that the subtransition temperature (now T_{CG} = 13.8 °C) occurs within 0.3 °C of the lower temperature found in both earlier equilibrium studies. Furthermore, there is only one apparent melting transition occurring in Figure 5 with a half-width of 0.3 °C. The only significant difference with the 1982 equilibrium dilatometric results is that the volume change is now ΔV = 0.017 mL/g compared to the 1982 value of 0.009 mL/g.

The reason that the dilatometry (and the adiabatic calorimetry) results in lower transition temperatures is simply that they were performed in equilibrium steps, whereas the DSC was performed at a scan rate of 13.6 °C/h. Figure 6 illustrates the effect of scan rate on the peak temperatures. Figure 6 also emphasizes the second point in Figure 5, namely, that the two apparently different subtransitions seen in Figure 2 are not seen when the melting is performed very slowly. As the scan rate is decreased, the two peaks merge into a single melting transition at 13.8 °C.

Figure 7 shows two hysteresis loops observed in the dilatometer. Each loop consists first of a cooling scan to the temperature of the lowest data point shown. As the lowest

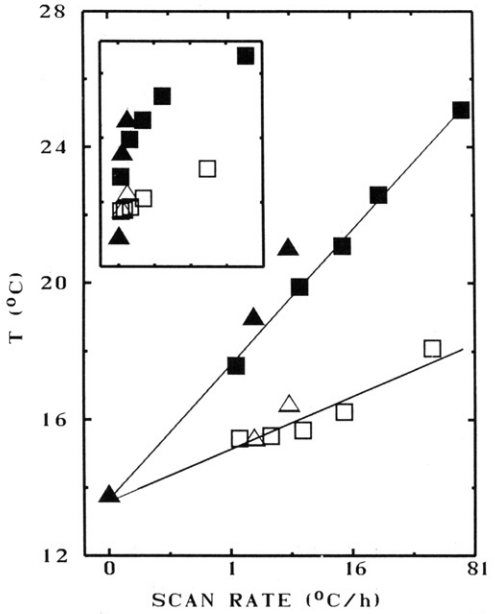

FIGURE 6: Vertical axis gives peak temperatures, T_{C^*G} (open symbols) and T_{CG} (closed symbols) (degrees centigrade). The horizontal axis is linear in the fourth root of the scanning rate (degrees centigrade per hour), and the numerical values on the graph are the actual scan rates. The squares were obtained from DSC, and the triangles were obtained from the dilatometer scans. The solid lines are the best linear least-squares fit to the DSC data. T_{C^*G} was determined for samples that had incubated for 1 day at 0.5 °C, and T_{CG} was determined for samples that had incubated for at least 15 days at 0.1–0.8 °C. The inset shows the same data plotted as a function of scan rate rather than as a function of the fourth root of the scan rate.

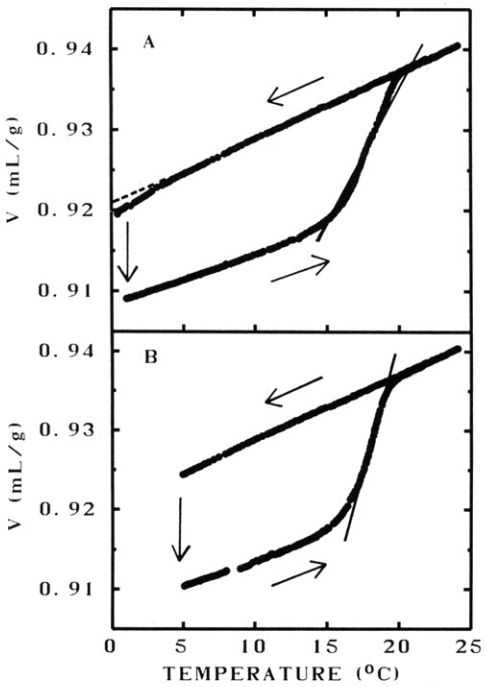

FIGURE 7: Hysteresis loops of absolute specific volumes (milliliters per gram) vs. temperature (degrees centigrade) with directions indicated by arrows. Cooling scans were performed at 2.8 °C/h, and heating scans were performed at 1.8 °C/h. Sample mass was 0.978 g of DPPC (75 mg/mL). (A) Sample was incubated for 15 days at 0.5 °C. (See curve A in Figure 8.) (B) Sample was incubated for 19 days at 4.9 °C. (See curve B in Figure 8.)

temperature in curve A is approached, it is clear that conversion into the C phase is already taking place, since the dashed line represents the extrapolated volume change using α_{gel}, the experimentally determined coefficient of expansion in the gel phase. The second part of the hysteresis loop is

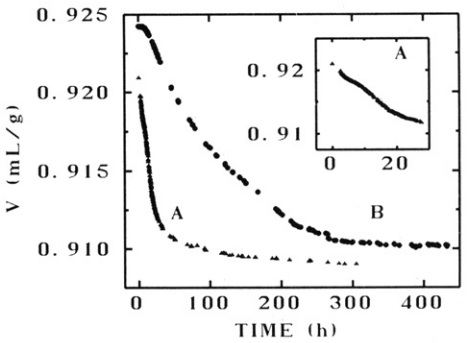

FIGURE 8: Absolute specific volumes (milliliters per gram) as a function of incubation time in hours for incubation temperatures (A) 0.5 and (B) 4.9 °C. Same sample as in Figure 7.

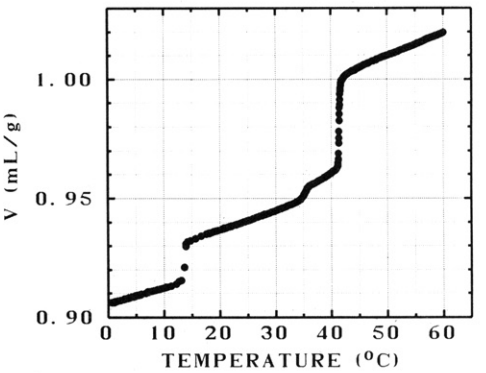

FIGURE 9: Absolute specific volumes (milliliters per gram) vs. temperature (degrees centigrade) of DPPC in all phases.

incubation of the sample at the lowest temperature shown. Finally, heating scans were performed on the dilatometer as shown in Figure 7.

Figure 8 shows the change in absolute specific volume as a function of time during the incubations that took place in Figure 7. For the lower incubation temperature (curve A in Figures 7 and 8), the volume initially decreased rapidly, then slowed perceptibly, and then decreased more rapidly (see the inset to Figure 8) before entering a regime of very slow volume decrease. This pattern, which was quite unexpected, was observed 3 times in three experiments. In one experiment, the incubation temperature was jumped from 0.8 °C after 96 h to 8.3 °C. After rapid equilibration to a larger volume compatible with the coefficient of expansion of the mixed C and G phases, the volume decreased, indicating continued conversion of the G phase to the C phase, with a faster rate than just before the temperature jump, consistent with earlier dilatometric results (Nagle & Wilkinson, 1982). At higher initial incubation temperatures, the volume decreased very little for 5–10 h, as seen in curve B in Figure 8, but then began to decrease more rapidly. The nearly linear ramp from about 70 to 200 h was observed twice in two experiments.

As seen in Figure 8, after 300–400 h of incubation, the rate of volume decrease becomes too slow for further monitoring on the dilatometer to be feasible. However, further slow volume decreases take place and were monitored by neutral flotation centrifugation for incubation periods up to 8 months. Using this technique, we found a final absolute specific volume of the C phase of 0.909 ± 0.001 mL/g at 5 °C. Together with the measured coefficient of volume expansion in the C phase which increases from (64 ± 4) × 10^{-5}/°C at 1 °C to (75 ± 1) × 10^{-5}/°C at 13 °C, the volume of the C phase at any temperature is obtained as shown in Figure 9, which also shows the absolute specific volumes of the higher temperature phases which are in agreement with earlier dilatometric results (Nagle

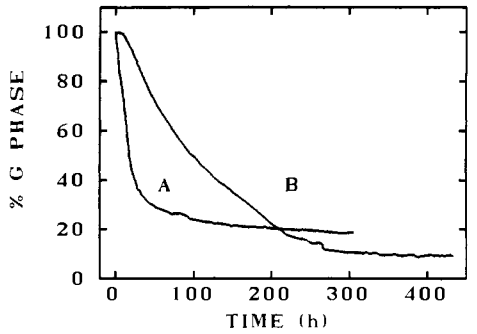

FIGURE 10: Extent of phase transformation from the G phase, where curve A (incubation temperature was 0.5 °C) and curve B (incubation temperature was 4.9 °C) correspond to the same data curves in Figure 8.

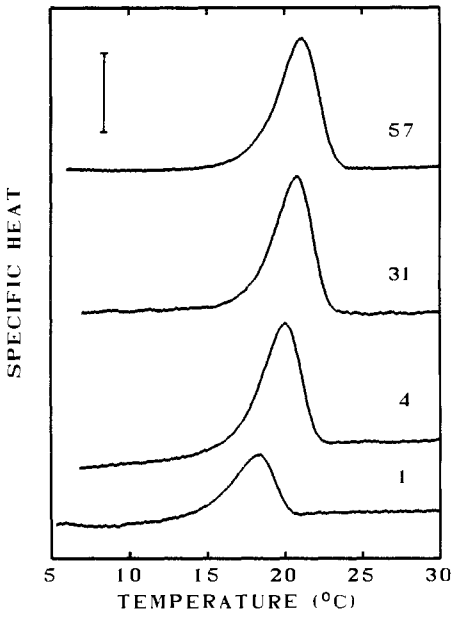

FIGURE 11: DSC scans of 3–5 mg/mL DPPC samples incubated at 4.6 °C for 1 day, ΔH = 2.1 kcal/mol; 4 days, ΔH = 4.0 kcal/mol; 31 days, ΔH = 4.1 kcal/mol; and 57 days, ΔH = 4.1 kcal/mol. Scan rate was 13.6 °C/h. The vertical bar indicates a specific heat of 1 cal/(deg·g).

& Wilkinson, 1978). From the results in Figure 9, the fractional completion of the phase transformation as a function of incubation time and temperature is easily obtained for any incubation temperature. As shown in Figure 10, after 300–400 h the extent of phase transformation was smaller when the sample was incubated at 0.5 °C instead of 4.9 °C despite the more rapid initial rate of conversion.

Returning to Figure 7, after the C phase was melted, the volume returned to its initial value, consistent with a return to the original G phase. As expected from the DSC results in Figures 2 and 6, the apparent melting transitions in Figure 7 occurred at elevated temperatures compared to the true T_{CG} = 13.8 °C obtained from equilibrium melting in Figure 5. Also, the melting curve A in Figure 7 for the sample incubated at 0.5 °C shows complex structure between 17 and 20 °C, with the solid lines representing the slopes at the midpoints. We interpret this as the dilatometric equivalent of the two peaks in the DSC performed at nonzero scanning rates. However, the sample incubated at 4.9 °C showed only one smooth melting curve (curve B in Figure 7). This latter result was then verified by using DSC; Figure 11 shows that there is only one endothermic peak, even when scanned at 13.6 °C/h, when the sample is incubated up to 57 days at 4.6 ± 0.2 °C. This result is in sharp contrast to the results shown in Figure 2 with

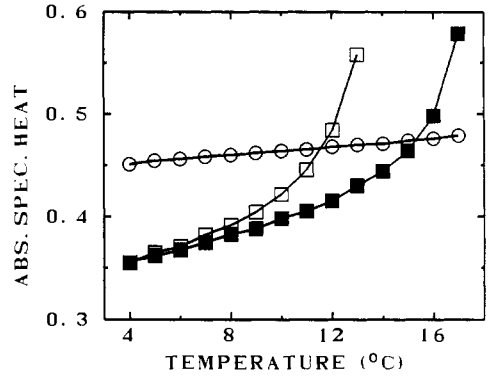

FIGURE 12: Absolute specific heat (calories per degree per gram) in the temperature region just below the subtransition for a 34.8-mg sample of DPPC was obtained as described by Wilkinson and Nagle (1982) and Tristram-Nagle et al. (1986). Closed squares show the specific heat after the sample had been incubated 4 months at 0.1 °C followed by 4 months at 4.6 °C. The open squares show the specific heat of the same sample after 1 day of incubation in the calorimeter at 2 ± 1 °C. After each scan of the subgel transition, the resulting unincubated sample was rescanned with the average result shown by circles. Scan rate was 13.1 °C/h.

the only difference in conditions being the incubation temperature.

In Figure 2, the slope in the DSC traces is larger for temperatures considerably below T_{C*G} and T_{CG} than for the single-phase gel region at temperatures above T_{CG}. This effect was investigated more thoroughly by using absolute specific heat measurements as shown in Figure 12. Even for temperatures as low as 4 °C, the slope is larger and the absolute specific heat is smaller when there is C or C* present than when there is just G present. Furthermore, even when the temperature of the subgel is raised to just below 13 °C, subsequent DSC scans from 0 °C still exhibit the upward slope (data not shown). However, as seen in Figure 11, when the C phase is formed at 4.6 °C at long incubation times, the slope below the subtransition is nearly the same as the slope in the gel phase. L. X. Finegold has also made DSC measurements with lower temperature startups that are consistent with the above results (personal communication).

Discussion

From the point of view of equilibrium thermodynamics, the multiple subtransition peaks so strikingly observed in DSC by ourselves (Figure 2) and others (Finegold & Singer, 1984; Wu et al., 1985; Silvius et al., 1985) are simply a kinetic artifact. Our equilibrium dilatometric measurements, shown in Figure 5, yield subgel melting at a single temperature whose value is in agreement with that measured by equilibrium adiabatic calorimetry (Kodama et al., 1985) and equilibrium dilatometry (Nagle & Wilkinson, 1982). As shown in Figure 6, the temperatures of the two peaks seen in nonequilibrium DSC (Figure 2) approach each other and the equilibrium temperature in a systematic way as the scanning rate is reduced. The insignificant difference between the molar values of ΔH_{C*G} and ΔH_{CG} obtained in Figure 3 also suggests that the putative C* and C phases are thermodynamically rather similar to each other. Clearly, one must be circumspect in interpreting multiple peaks observed by DSC scans which are fast compared to the time constant for the transition. Furthermore, in order to obtain accurate transition temperatures, data should be taken at different scan rates to determine if there is a scan rate dependence and to allow an extrapolation to zero scan rate in lieu of an equilibrium measurement. Nevertheless, it is also of interest to understand what causes the kind of kinetic

behavior that appears in Figure 2. For this, it will be convenient to retain the notation C* to indicate a metastable phase, both upon formation and upon melting.

The usual picture of the kinetics of transformations into more ordered phases is that nuclei of the new phase must first be formed. Even though the new phase is the stable phase, very small nuclei of the new phase are unstable because of the domain wall energy (Dunning, 1969). Only when thermal fluctuations create nuclei of the new phase that are large enough to be stable will irreversible growth of the new phase occur. Therefore, it is conventional to separate the transformation into two steps, nucleation and growth. Of course, if the nucleation step is very fast, then it will not be the rate-limiting step and will not be apparent. This appears to have been the case in earlier studies (Nagle & Wilkinson, 1982) and also in the data taken at the lower incubation temperatures, curve A in Figure 8. However, the data taken at the higher incubation temperature in Figure 8 (curve B) show a "lag time" effect in that the volume change is small at initial times compared to later times. We interpret the lag time roughly as the time that it takes nuclei to form before growth can occur. According to classical homogeneous nucleation theory (Dunning, 1969), the lag time due to nucleation will be longer the closer the temperature is to the equilibrium transition temperature, so this picture of the subgel phase transformation appears to provide a qualitative interpretation of our data in Figure 8.

Figure 10 shows that the extent of phase transformation is higher after 300-h incubation when the incubation temperature is higher (4.9 °C), even though the initial rate of transformation is higher for the lower incubation temperature (0.5 °C). Figure 11 also shows that incubation at higher temperatures results in simpler melting peaks with transition enthalpies as large as the ΔH_{CG} obtained by extrapolating to $t = \infty$. Also, for higher incubation temperatures, the absolute specific heat behaves more normally below the subgel transition, and the melting temperatures approach more rapidly those of the C phase shown in Figure 2. These results encourage us to suggest that the preferred incubation conditions for the C phase involve higher incubation temperatures, since more complete transformation into the most stable C phase then occurs.

In addition to the above suggestion, we propose a theory that accounts for the experimental results that led to it. We begin to develop this theory by considering the formation kinetics. At low incubation temperatures (about 0.5 °C), many nuclei form quickly and proceed to grow. Since the mean distance between nucleation centers is small, the domains collide when the average domain size is small. Since each domain will be oriented randomly within the plane of the membrane with respect to a neighboring domain, the collision region, i.e., the domain wall region, will involve mismatches or defects which will not have as small a volume as the perfect C phase. These imperfect regions will only gradually anneal into more perfect, high-density material; this gradualness is consistent with the very slow decay seen at long times in the formation kinetics shown in curve A in Figures 8 and 10. In contrast, at higher incubation temperatures (about 5 °C), the mean distance between nuclei is greater. Once a nucleus is formed, it can grow into a larger C-phase domain. Since the amount of low-density domain wall material is smaller in this case, the amplitude of the slower annealing transformation would be smaller. A clear manifestation of the greater extent of phase transformation is seen in curve B in Figure 10 when compared to curve A at 300 h. Of course, the initial rates of volume decrease are faster at low incubation temperatures because the rate of nucleation is much faster.

Now consider the melting kinetics. Melting usually is initiated at the defects in crystals, so in this theory melting may begin at the domain wall boundaries and proceed inward into the C-phase domains. However, melting may also begin at other imperfections that will inevitably be present even in large C-phase domains that are grown from a single nucleus. This latter mechanism will be the dominant one for melting when the domains are large. As the domain size decreases, the domain wall melting mechanism will become dominant, and the melting will occur more quickly, that is, at lower temperatures in DSC scans. These considerations suggest that perhaps the CG peaks in the DSC scans in Figure 2 and in Figure 11 are due to the melting of large domains and the C*G peaks in Figure 2 are due to the melting of smaller domains separated by low-density domain walls that initiate the melting. If so, then there is no intrinsic difference between the C* and the C "phases" except for the domain wall pattern which may be changed by the degree of annealing and the method of formation. This view is consistent with the $\Delta H(\infty)$ being very close for the two phases, with ΔH_{C^*G} being slightly smaller than ΔH_{CG} because the domain wall region would still be somewhat disordered. It is also consistent with the result in Figure 5 that the melting exhibits only a single peak when performed in equilibrium.

An additional perspective concerns the amount of water in the subgel phase, which Ruocco and Shipley (1982b) found to be reduced (11 water molecules/lipid) from 19 water molecules/lipid in the gel phase. These authors suggested that there are two kinetic steps in the formation of the subgel. At −2 °C incubation, the first step involves a fast crystalline reordering of the hydrocarbon chains seen by rapid changes in the wide-angle diffraction spacing that slow markedly after 2 h. The second step involves the loss of some of the water molecules from the interlamellar region monitored by the d spacing (starting about 2 h) that appears to trigger further reordering of the hydrocarbon chains into the C phase (5 h later). One might interpret the delay in the final reordering of the chains to be caused by the presence of too much water between the bilayers. A strikingly similar delay in the volume decrease upon incubation at 0.5 °C is seen in our Figure 8A (inset) between 5- and 10-h incubation, the time being somewhat later due to the higher incubation temperature. Thus, in the time required for C* formation, dehydration of the bilayers may be temporarily rate limiting. This leads us to suggest that on a longer time scale the loss of the final water molecules may also become rate limiting for C* to C conversion. The experimental results shown in Figure 4 support this hypothesis. We observed that the kinetics of formation of the CG peak are slowed by a factor of roughly 2 when D_2O is substituted for H_2O. This may be due to a slower diffusion constant of D_2O through lipid bilayers by a factor of 1.6 ± 0.4 (Bittman & Blau, 1972). When incubation is carried out at 4.9 °C, the delay in the volume decrease occurs at about 70 h and is not so apparent. In this case, it is possible that the diffusion of water through the bilayer proceeds at a comparable rate to subgel formation. This is in agreement with an equilibration time τ of 50 h for water diffusing through liposomes of size $r = 1$ μm using the formula $2D\tau = r^2$ and the measured permeabilities of water through lipid bilayers in the gel phase (Carruthers & Melchior, 1983).

We have no fully satisfactory explanation for the greater slope of the specific heat below the subgel transition seen in Figures 2 and 12. It may, however, be useful to mention two hypotheses that do not appear to work. At first, the greater

slope is reminiscent of the increasing slope that is also seen in the gel phase, and that has been explained as the effect of hindered vibrations (Wilkinson & Nagle, 1982). However, the slope in the subgel phase in Figures 2 and 12 is much larger than the slope in the gel phase. The fact that this slope clearly depends upon incubation conditions, as seen in Figures 2 and 11, and becomes smaller under those conditions when the C phase is most perfectly formed is difficult to reconcile with the hindered vibration hypothesis. The second hypothesis invokes the annealing out of defects or, in those experiments in which conversion to the subgel phase is not complete, the continued growth of the subgel phase during the heating scan. Since both processes are exothermic, this hypothesis is consistent with the fact that the absolute specific heat is smaller below the subgel transition in those samples that have the large slope in specific heat. However, this hypothesis is inconsistent with the observation that the specific heat is unchanged when a scan terminated at 13 °C is followed by a second scan from 4 °C, because the exothermic annealing that would lower the specific heat in the first scan should not occur to as large an extent in the rescan. Although we wish that we understood this effect better, it is nevertheless encouraging that it does not occur for the samples that we believe to be the best representatives of the pure C phase, namely, those that have been incubated for the longest times at the warmer incubation temperatures such as the 57-day curve in Figure 11.

ACKNOWLEDGMENTS

We thank Prof. L. X. Finegold for helpful discussions and for communicating his DSC data.

Registry No. DPPC, 63-89-8.

REFERENCES

Bittman, R., & Blau, L. (1972) *Biochemistry 11*, 4831–4839.
Blaurock, A. E., & McIntosh, T. J. (1986) *Biochemistry 25*, 299–305.
Cameron, D. G., & Mantsch, H. H. (1982) *Biophys. J. 38*, 175–184.
Carruthers, A., & Melchior, D. L. (1983) *Biochemistry 22*, 5797–5807.
Chen, S. C., Sturtevant, J. M., & Gaffney, B. J. (1980) *Proc. Natl. Acad. Sci. U.S.A. 77*, 5060–5063.
Church, S. E., Griffiths, D. J., Lewis, R. N. A. H., McElhaney, R. N., & Wickman, H. H. (1986) *Biophys. J. 49*, 597–605.
Dunning, W. J. (1969) in *Nucleation* (Zettlemoyer, A. C., Ed.) pp 1–67, Marcel Dekker, New York.
Finegold, L., & Singer, M. A. (1984) *Chem. Phys. Lipids 35*, 291–297.
Finegold, L., & Singer, M. A. (1986) *Biochim. Biophys. Acta 855*, 417–420.
Fuldner, H. H. (1981) *Biochemistry 20*, 5707–5710.
Kodama, M., Hashigami, H., & Seki, S. (1985) *Biochim. Biophys. Acta 814*, 300–306.
McIntosh, T. J., & Simon, S. A. (1986) *Biochemistry 25*, 4948–4952.
Nagle, J. F., & Wilkinson, D. A. (1978) *Biophys. J. 23*, 159–175.
Nagle, J. F., & Wilkinson, D. A. (1982) *Biochemistry 21*, 3817–3821.
Ruocco, M. J., & Shipley, G. G. (1982a) *Biochim. Biophys. Acta 684*, 59–66.
Ruocco, M. J., & Shipley, G. G. (1982b) *Biochim. Biophys. Acta 691*, 309–320.
Serrallach, E. N., deHaas, G. H., & Shipley, G. G. (1984) *Biochemistry 23*, 713–720.
Silvius, J. R., Lyons, M., Yeagle, P. L., & O'Leary, T. J. (1985) *Biochemistry 24*, 5388–5395.
Singer, M. A., & Finegold, L. (1985) *Biochim. Biophys. Acta 816*, 303–312.
Ter-Minassian-Saraga, L., & Madelmont, G. (1984) *J. Colloid Interface Sci. 99*, 420–426.
Tristram-Nagle, S., & Nagle, J. F. (1986) *Biophys. J. 49*, 506a.
Tristram-Nagle, S., Yang, C.-P., & Nagle, J. F. (1986) *Biochim. Biophys. Acta 854*, 58–66.
Wiener, M. C., Tristram-Nagle, S., & Nagle, J. F. (1987) *Biophys. J. 51*, 159a.
Wilkinson, D. A., & Nagle, J. F. (1978) *Anal. Biochem. 84*, 263–271.
Wilkinson, D. A., & Nagle, J. F. (1982) *Biochim. Biophys. Acta 688*, 107–115.
Wilkinson, D. A., & McIntosh, T. J. (1986) *Biochemistry 25*, 295–298.
Wu, W.-G., Chong, L.-G., & Huang, C.-H. (1985) *Biophys. J. 47*, 237–242.
Yang, C.-P., Wiener, M. C., Lewis, R. N. A. H., McElhaney, R. N., & Nagle, J. F. (1986) *Biochim. Biophys. Acta 863*, 33.